

# A series of nanometer-sized hexanuclear Co-, Fe-, and Ga-metallamacrocycles

Inhoe Kim, Byunghoon Kwak, Myoung Soo Lah \*

*Department of Chemistry, College of Science, Hanyang University, 1271 Sa-1-dong, Ansan, Kyunggi-do 425-791, South Korea*

Received 7 July 2000; accepted 2 February 2001

## Abstract

In this study, we expanded a manganese ion in metallamacrocycles to the other octahedral transition metal ions with +3 oxidation states. A series of nanometer-sized hexanuclear cobalt-, iron-, and gallium-metallamacrocycles were synthesized using pentadentate ligands (*N*-acetylsalicylhydrazides ( $H_3xshz$ ) (*N*-formylsalicylhydrazide,  $H_3fshz$ ; *N*-acetylsalicylhydrazide,  $H_3ashz$ ; *N*-propionylsalicylhydrazide,  $H_3pshz$ ; *N*-hexanoylsalicylhydrazide,  $H_3hshz$ ; *N*-lauroylsalicylhydrazide,  $H_3lshz$ ). The triple-deprotonated *N*-acetylsalicylhydrazidate ( $xshz^{3-}$ ) bridged the metal ions using a hydrazide N–N group and formed the hexanuclear metallamacrocycles. All hexanuclear metallamacrocycles with various kinds of metal ions and a series of pentadentate ligands are isostructural. The formation of the hexanuclear metallamacrocycles is unaffected not only by the introduction of alkyl side chains in the pentadentate ligands, but also by substituting the manganese ion with other octahedral transition metal ions such as cobalt, iron and gallium. The presence of a replaceable solvent site in the metal center indicates that the hexanuclear metallamacrocycles could be used as secondary building units for the synthesis of open frameworks with various active metal sites. © 2001 Elsevier Science B.V. All rights reserved.

*Keywords:* Crystal structures; Cobalt complexes; Iron complexes; Metallamacrocycles

## 1. Introduction

Coordination chemistry is an emerging tool for the construction of organized supramolecular structures [1]. The main strategy for the construction of the supramolecular structures is the self-assembly of the appropriate metal ions and a tailored ligand in an appropriate solvent. Depending on the intrinsic properties of the metal ions and the ligands used, one-dimensional [2], two-dimensional [3] or three-dimensional network structures [4,5] could be assembled. The ability to control the supramolecular structures with desired structures and properties is still a substantial challenge. The generation of a large void space is a difficult task due to nature's tendency to avoid a vacuum. The void space in the networks has usually been filled by the

interpenetration of identical copies [5]. A new strategy for the construction of a microporous material is to use inorganic clusters as secondary building units in the assembly of the extended networks [6]. We have recently synthesized a series of nanometer-sized hexanuclear manganese-metallamacrocycles using chelating pentadentate ligands [7]. In addition, we were able to synthesize three-dimensional open framework using a hexanuclear manganese metallamacrocycle as a nanoscale secondary building unit [8]. Interestingly, some of the metal centers in an open framework are exposed in the porous channels and the metal centers were able to be used as active sites for recognition of the guest molecule.

In this study, we expanded on the manganese ion containing hexanuclear metallamacrocycles to cover other octahedral transition metal ion containing hexanuclear metallamacrocycles. We synthesized and characterized a series of cobalt, iron and gallium metallamacrocycles.

\* Corresponding author. Tel.: +82-31-400 5496; fax: +82-31-407 3863.

*E-mail address:* mslah@hanyang.ac.kr (Myoung Soo Lah).

## 2. Experimental

### 2.1. Materials

The following were used as received with no further purification: gallium(III) nitrate hydrate, cobalt(II) acetate tetrahydrate and iron(II) chloride tetrahydrate from Aldrich, Inc.; methanol (MeOH), ethanol (EtOH) and dimethylformamide (DMF) from Carlo Erba. A series of potential pentadentate ligands, *N*-acetylsalicylhydrazides ( $H_3xshz$ ) (*N*-formylsalicylhydrazide:  $H_3fshz$ ; *N*-acetylsalicylhydrazide:  $H_3ashz$ ; *N*-propionylsalicylhydrazide:  $H_3pshz$ ; *N*-hexanoylsalicylhydrazide:  $H_3hshz$ ; *N*-lauroylsalicylhydrazide:  $H_3lshz$ ) were synthesized by coupling of the salicylhydrazide and the corresponding acyl chloride or acyl anhydrides [7].

### 2.2. Instrumentation

**Elemental Analysis:** The Elemental Analysis Laboratory of the Korean Institute of Basic Science performed C, H, N, Co, Fe and Ga determinations. **IR spectra:** Infrared spectra were recorded as KBr pellets in the range 4000–600  $cm^{-1}$  on a BioRad FT IR spectrometer. **Absorption Spectra:** Absorption spectra were obtained using a Perkin–Elmer Lambda spectrometer.

### 2.3. Synthesis

#### 2.3.1. Synthesis of cobalt-metallamacrocycles

$[Co(fshz)(MeOH)]_6$  (**1**). A 0.364 g (2.0 mmol) sample of  $H_3fshz$  was dissolved in 30 ml of MeOH, and 0.498 g (2.0 mmol) of cobalt(II) acetate tetrahydrate was dissolved in 30 ml of MeOH in another flask. The two solutions were mixed, and the combined solution was allowed to stand for a week, whereupon dark purple crystals were obtained (0.496 g, 90.1% yield). *Anal.* Found: C, 34.90; H, 3.79; Co, 21.90; N, 9.44. Calc. for  $[Co(fshz)(H_2O)]_6 \cdot 7H_2O$  ( $Co_6C_{48}H_{56}N_{12}O_{31}$ ) (FW = 1650.63): C, 34.93; H, 3.42; Co, 21.42; N, 10.18%. UV–Vis:  $\lambda_{max}$  (nm) ( $\epsilon$ ,  $M^{-1}cm^{-1}$ ) (DMF) 298 (16 800), 366 (14 300).

$[Co(ashz)(MeOH)]_6$  (**2**). Complex **2** was prepared in an analogous manner to that used for the complex **1** using: a 0.194 g (1.0 mmol) sample of  $H_3ashz$  in 10 ml of MeOH, and 0.249 g (1.0 mmol) of cobalt(II) acetate tetrahydrate in 10 ml of MeOH (0.243 g, 84.0% yield). *Anal.* Found: C, 37.71; H, 4.22; Co, 20.8; N, 9.36. Calc. for  $[Co(ashz)(H_2O)]_6 \cdot 7H_2O$  ( $Co_6C_{54}H_{68}N_{12}O_{31}$ ) (FW = 1734.79): C, 37.39; H, 3.95; Co, 20.38; N, 9.69%.

$[Co(pshz)(MeOH)]_6$  (**3**). Complex **3** was prepared in an analogous manner to that used for the complex **1** using: a 0.208 g (1.0 mmol) sample of  $H_3pshz$  in 10 ml of MeOH, and 0.249 g (1.0 mmol) of cobalt(II) acetate tetrahydrate in 10 ml of MeOH (0.238 g, 84.4% yield). *Anal.* Found: C, 43.13; H, 4.20; Co, 21.1; N, 9.72. Calc.

for  $[Co(pshz)(H_2O)]_6$  ( $Co_6C_{72}H_{90}N_{12}O_{24}$ ) (FW = 1692.85): C, 42.57; H, 3.93; Co, 20.89; N, 9.93%.

$[Co(hshz)(MeOH)]_6$  (**4**). Complex **4** was prepared in an analogous manner to that used for the complex **1** using: a 0.250 g (1.0 mmol) sample of  $H_3hshz$  in 10 ml of MeOH, and 0.249 g (1.0 mmol) of cobalt(II) acetate tetrahydrate in 10 ml of MeOH (0.279 g, 86.0% yield). *Anal.* Found: C, 49.17; H, 5.03; Co, 18.9; N, 8.65. Calc. for  $[Co(hshz)(H_2O)]_6$  ( $Co_6C_{78}H_{102}N_{12}O_{24}$ ) (FW = 1945.33): C, 48.16; H, 5.28; Co, 18.18; N, 8.64%.

$[Co(lshz)(MeOH)]_6$  (**5**). Complex **5** was prepared in an analogous manner to that used for the complex **1** using: a 0.334 g (1.0 mmol) sample of  $H_3lshz$  in 10 ml of MeOH, and 0.249 g (1.0 mmol) of cobalt(II) acetate tetrahydrate in 10 ml of MeOH (0.398 g, 97.5% yield). *Anal.* Found: C, 56.24; H, 6.82; Co, 14.8; N, 6.76. Calc. for  $[Co(lshz)(H_2O)]_6$  ( $Co_6C_{114}H_{174}N_{12}O_{24}$ ) (FW = 2450.30): C, 55.88; H, 7.16; Co, 14.43; N, 6.86%.

#### 2.3.2. Synthesis of iron-metallamacrocycles

$[Fe(ashz)(DMF)]_6$  (**6**). A 0.194 g (1.0 mmol) sample of  $H_3ashz$  was dissolved in 15 ml of DMF, and 0.199 g (1.0 mmol) of iron(II) chloride tetrahydrate was dissolved in 15 ml of DMF in another flask. The two solutions were mixed, and the combined solution was allowed to stand for 10 days, whereupon dark brown crystals were obtained (0.133 g, 46.0% yield). *Anal.* Found: C, 41.10; H, 4.01; Fe, 19.8; N, 11.43. Calc. for  $[Fe_6(ashz)_6(DMF)_2(H_2O)_4] \cdot 2H_2O$  ( $Fe_6C_{60}H_{68}N_{14}O_{26}$ ) (FW = 1736.36): C, 41.50; H, 3.95; Fe, 19.30; N, 11.29%.

$[Fe(pshz)(DMF)]_6$  (**7**). A 0.416 g (2.0 mmol) sample of  $H_3pshz$  was dissolved in 20 ml of DMF for 5 min, then 0.398 g (2.0 mmol) of iron(II) chloride tetrahydrate was added to the solution. The solution was allowed to stand for 10 days, whereupon dark brown crystals were obtained (0.110 g, 28.1% yield). *Anal.* Found: C, 43.81; H, 4.83; Fe, 18.7; N, 11.61. Calc. for  $[Fe_6(pshz)_6(DMF)_2(H_2O)_4] \cdot H_2O$  ( $Fe_6C_{66}H_{78}N_{14}O_{25}$ ) (FW = 1802.51): C, 43.98; H, 4.36; Fe, 18.59; N, 10.88%.

$[Fe(hshz)(DMF)]_6$  (**8**). Complex **8** was prepared in an analogous manner to that used for the complex **6** using: a 0.500 g (2.0 mmol) sample of  $H_3hshz$  in 10 ml of DMF, and 0.398 g (2.0 mmol) of iron(II) chloride tetrahydrate in 10 ml of DMF (0.625 g, 83.1% yield). *Anal.* Found: C, 50.71; H, 5.23; Fe, 14.8; N, 11.04. Calc. for  $[Fe(hshz)(DMF)]_6$  ( $Fe_6C_{96}H_{132}N_{18}O_{24}$ ) (FW = 2257.29): C, 51.08; H, 5.89; Fe, 14.84; N, 11.17%.

$[Fe(lshz)(DMF)]_6$  (**9**). Complex **9** was prepared in an analogous manner to that used for the complex **6** using: a 0.334 g (1.0 mmol) sample of  $H_3lshz$  in 15 ml of DMF, and 0.199 g (1.0 mmol) of iron(II) chloride tetrahydrate in 15 ml of DMF (0.364 g, 82.9% yield). *Anal.* Found: C, 55.98; H, 6.65; Fe, 12.8; N, 8.44. Calc. for  $[Fe_6(lshz)_6(DMF)_3(H_2O)_3] \cdot 2H_2O$

( $\text{Fe}_6\text{C}_{123}\text{H}_{193}\text{N}_{15}\text{O}_{26}$ ) (FW = 2633.05): C, 56.11; H, 7.39; Fe, 12.73; N, 7.98%.

### 2.3.3. Synthesis of gallium-metallamacrocycles

[Ga(fshz)(EtOH)]<sub>6</sub> (**10**). A 0.182 g (1.0 mmol) sample of H<sub>3</sub>fshz was dissolved in 5 ml of EtOH, and 0.256 g (1.0 mmol) of gallium (III) nitrate hydrate was added. The two solutions were mixed, and the combined solution was allowed to stand for a week, whereupon white transparent crystals were obtained (0.176 g, 60.3% yield). *Anal.* Found: C, 32.43; H, 3.45; Ga, 24.1; N, 9.60. Calc. for [Ga(fshz)(H<sub>2</sub>O)]<sub>6</sub>·9H<sub>2</sub>O (Ga<sub>6</sub>C<sub>48</sub>H<sub>60</sub>N<sub>12</sub>O<sub>33</sub>) (FW = 1751.39): C, 32.92; H, 3.45; Ga, 23.89; N, 9.60%.

[Ga(ashz)(MeOH)]<sub>6</sub> (**11**). Complex **11** was prepared in an analogous manner to that used for the complex **10** using: a 0.191 g (1.0 mmol) sample of H<sub>3</sub>ashz in 5 ml of MeOH, and 0.255 g (1.0 mmol) of gallium (III) nitrate hydrate in 10 ml of MeOH (0.17 g, 57.3% yield). *Anal.* Found: C, 36.90; H, 4.33; Ga, 23.03; N, 9.07. Calc. for [Ga(ashz)(H<sub>2</sub>O)]<sub>6</sub>·6H<sub>2</sub>O (Ga<sub>6</sub>C<sub>54</sub>H<sub>66</sub>N<sub>12</sub>O<sub>30</sub>) (FW = 1781.50): C, 36.41; H, 3.73; Ga, 23.48; N, 9.43%.

[Ga(pshz)(EtOH)]<sub>6</sub> (**12**). Complex **12** was prepared in an analogous manner to that used for the complex **10** using: a 0.210 g (1.0 mmol) sample of H<sub>3</sub>pshz in 10 ml of EtOH, and 0.49 g (2 mmol) of gallium(III) nitrate hydrate in 5 ml of EtOH (0.18 g, 61.4% yield). *Anal.* Found: C, 41.10; H, 4.77; Ga, 23.57; N, 8.31. Calc. for [Ga(pshz)(H<sub>2</sub>O)]<sub>6</sub> (Ga<sub>6</sub>C<sub>60</sub>H<sub>66</sub>N<sub>12</sub>O<sub>24</sub>) (FW = 1757.57): C, 41.10; H, 3.80; Ga, 23.60; N, 9.59%.

[Ga(hshz)(EtOH)]<sub>6</sub> (**13**). The complex **13** was prepared in an analogous manner to that used for the complex **10** using: a 0.260 g (1.0 mmol) sample of H<sub>3</sub>hshz in 10 ml of EtOH, and 0.256 g (1.0 mmol) of gallium(III) nitrate hydrate in 10 ml of EtOH (0.26 g, 71.8% yield). *Anal.* Found: C, 43.11; H, 5.57; Ga, 19.7; N, 7.74. Calc. for [Ga(hshz)(H<sub>2</sub>O)]<sub>6</sub>·9H<sub>2</sub>O (Ga<sub>6</sub>C<sub>78</sub>H<sub>102</sub>N<sub>12</sub>O<sub>33</sub>) (FW = 2172.19): C, 43.13; H, 5.57; Ga, 19.26; N, 7.74%.

[Ga(lshz)(EtOH)]<sub>6</sub> (**14**). The complex **14** was prepared in an analogous manner to that used for the complex **10** using: a 0.300 g (1.0 mmol) sample of H<sub>3</sub>lshz in 20 ml of EtOH–CH<sub>2</sub>Cl<sub>2</sub> mixed solvent, and 0.256 g (1.0 mmol) of gallium(III) nitrate hydrate in 10 ml of EtOH (0.36 g, 80.5% yield). *Anal.* Found: C, 56.24; H, 7.29; Ga, 15.4; N, 6.67. Calc. for [Ga(lshz)(EtOH)]<sub>6</sub> (Ga<sub>6</sub>C<sub>126</sub>H<sub>198</sub>N<sub>12</sub>O<sub>24</sub>) (FW = 2683.34): C, 56.40; H, 7.44; Ga, 15.59; N, 6.26%.

## 2.4. Crystallographic data collection and refinement of structures

Because all crystals lose their structural solvents of crystallization within a few minutes, they were mounted in a glass capillary with the mother liquor to prevent the loss of the structural solvents during data collec-

tion. Preliminary examination and data collection for all crystals were performed with Mo K $\alpha$  radiation ( $\lambda = 0.71069 \text{ \AA}$ ) on an Enraf–Nonius CAD-4 computer-controlled  $\kappa$ -axis diffractometer equipped with a graphite crystal, incident-beam monochromator. Cell constants and orientation matrices for data collection were obtained from least-squares refinement, using the setting angles of 25 reflections. Data were collected at room temperature using the  $\omega$ -scan technique. Three standard reflections were monitored every hour, but no intensity variations were monitored. Lorentz and polarization corrections were applied to the data; however, no corrections were made for absorption. All structures were solved by direct methods using SHELXS-86 [9] and refined by full-matrix least-squares calculations with SHELX-97 [10].

*Complex [Co(fshz)(MeOH)]<sub>6</sub> (**1**)*. All non-hydrogen atoms were refined anisotropically; hydrogen atoms were allowed to ride on geometrically ideal positions with isotropic temperature factors 1.2 times those of the attached non-hydrogen atoms. Three solvent sites were observed and two of them are statistically disordered.

*Complex [Fe(ashz)(DMF)]<sub>6</sub> (**6**)*. More than ten non-coordinating solvent sites were observed in the solvent area. However, several of them were disordered or partly resolved. Refinement of the structure with approximate positions of disordered or partly resolved DMF molecules converged at final  $R_1 = 0.1146$  for 5232 reflections of  $I > 2\sigma(I)$ ,  $R_1 = 0.2139$ ,  $wR_2 = 0.3634$  for all 15 196 reflections. The volume occupied by the non-coordinating solvent molecules was estimated to be about 35% of the crystal volume by the PLATON program [11]. Structure refinement without non-coordinating solvent molecules following modification of the data with the SQUEEZE routine led to better refinement than when all of the solvent molecules were included in modeling of the raw data. This refinement converged at final  $R_1 = 0.1093$  for 5802 reflections of  $I > 2\sigma(I)$ ,  $R_1 = 0.1678$ ,  $wR_2 = 0.3063$  for all 15 196 reflections.

*Complex [Fe(pshz)(DMF)]<sub>6</sub> (**7**)*. All non-hydrogen atoms were refined anisotropically; hydrogen atoms were allowed to ride on geometrically ideal positions with isotropic temperature factors 1.2 times those of the attached non-hydrogen atoms. The solvent molecule coordinated to metal ion was treated as a disordered DMF molecule where the remaining non-hydrogen atoms of the DMF molecule were disordered. This molecule also could be treated as a water molecule because only one non-hydrogen atom was observed around the solvent site. Three additional solvent sites were identified but all of them statistically disordered.

*Complex [Fe(hshz)(DMF)]<sub>6</sub> (**8**)*. In the refinement of crystal **8**, three pentyl side chains of the ligands and the two of the three coordinated solvent molecules were disordered. During the least-squares refinement of crystal **8**, all alkyl side chains of the ligands were restrained as an ideal geometry.

**Complex  $[Ga(fshz)(EtOH)]_6$  (10).** Only the metal ions were refined anisotropically; hydrogen atoms were allowed to ride on geometrically ideal positions with isotropic temperature factors 1.2 times those of the attached non-hydrogen atoms. More than 15 non-coordinating solvent sites were observed in the solvent area. However, several of them were partly resolved.

**Complex  $[Ga(ashz)(MeOH)]_6$  (11).** All non-hydrogen atoms were refined anisotropically; hydrogen atoms were allowed to ride on geometrically ideal positions with isotropic temperature factors 1.2 times those of the attached non-hydrogen atoms. Six solvent sites were identified but two of them were statistically disordered.

**Complex  $[Ga(pshz)(EtOH)]_6$  (12).** Only the metal ions were refined anisotropically; hydrogen atoms were allowed to ride on geometrically ideal positions with isotropic temperature factors 1.2 times those of the attached non-hydrogen atoms. Three solvent molecules were identified.

**Complex  $[Ga(lshz)(EtOH)]_6$  (14).** All non-hydrogen atoms were refined anisotropically; hydrogen atoms were allowed to ride on geometrically ideal positions with isotropic temperature factors 1.2 times those of the attached non-hydrogen atoms. In the refinement of crystal **14**, two lauroyl side chains of the ligands were disordered. During the least-squares refinement of crystal **14**, the disordered alkyl side chains of the ligands were restrained as an ideal geometry.

Crystal and intensity data are given in Table 1.

### 3. Results and discussion

#### 3.1. Synthesis of metallamacrocycles

The general reaction scheme for the preparation of metallamacrocycles, applicable in coordinating solvents MeOH, EtOH or DMF, is given in Scheme 1.

The final oxidation state of the metal ions was not dictated by the initial metal ion source since the metals

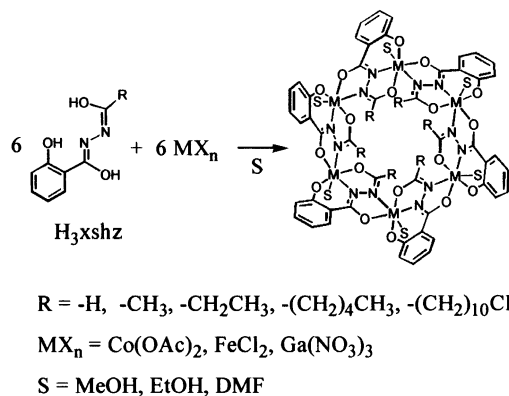
are oxidized aerobically to a +3 oxidation state. The potential trianionic pentadentate ligand,  $H_3xshz$ , bridges the metal ions to form a 24-membered hexanuclear metallamacrocycle. The triple-deprotonated *N*-acylsalicylhydrazidate ( $xshz^{3-}$ ) with a linear aliphatic chain could bridge the metal ions using a hydrazide N–N group and form the isostructural hexanuclear metallamacrocycle.

#### 3.2. Structural overview of metallamacrocycles

All hexanuclear metallamacrocycles are similar to the previously reported hexanuclear manganese-metallamacrocycles [7]. Metallamacrocycles with six ring metal ions have non-crystallographic  $S_6$  symmetry. The pentadentate ligand *N*-acylsalicylhydrazidate bridges the ring metal ions using a hydrazide N–N group. An iminophenolate group (O1 and N1 atoms) and an iminoacyl group (N1 and O3 atoms) of the ligand are coordinated to the metal ion in the meridional mode to form the six-membered and five-membered chelating rings. A hydrazidate group (O2 and N2 atoms) occupies two of the three remaining coordination sites of the octahedral metal ions to form the five-membered chelating ring. A monodentate solvent molecule finishes the octahedral geometry of the tricationic metal ion. The binding mode of the ligand enforces the stereochemistry of the metal ions only into a propeller configuration. The resulting chiralities of the metal centers in metallamacrocycles alternate between  $\Lambda$  and  $\Delta$  forms. The alternations of the chiralities of the metal centers expand the cyclic ring system of the metallamacrocycle to the 24-membered ring system. The cores of the all disc-shaped hexanuclear metallamacrocycles are approximately 2 nm in diameter and 1 nm in thickness. Even though the overall shape of the metallamacrocycles is disc-shaped, the six ring metal ions are not in a plane (Table 3). The six ring metal ions are in chair conformation.

##### 3.2.1. Cobalt-metallamacrocycles

**Crystal structure of  $[Co(fshz)(MeOH)]_6$  (1).** A hexanuclear cobalt-metallamacrocycle **1** could be synthesized using cobalt(II) acetate tetrahydrate as the metal source and  $fshz^{3-}$  as a trianionic pentadentate ligand. An ORTEP diagram of complex **1** is shown in Fig. 1. This neutral hexanuclear cobalt-metallamacrocycle is similar to the previously reported hexanuclear manganese-metallamacrocycle  $[Mn(fshz)(DMF)]_6$  (**15**) (Tables 2 and 3) [7a]. Complex **1** with non-crystallographic local pseudo- $C_{3i}$  symmetry is in the crystallographic inversion center. The approximate dimensions of the disk-shaped cobalt-metallamacrocycle (16.6 Å in diameter) are a little smaller than that of the corresponding manganese complex  $[Mn(fshz)(DMF)]_6$  (17.7 Å in diameter). Complex **1** has a small vacant, hydrophobic



Scheme 1.

Table 1  
Crystal data for Co-metallamacrocycles **1**; and Fe-metallamacrocycles **6–8**; Ga-metallamacrocycles **10–12** and **14**

Complex	<b>1</b>	<b>6</b>	<b>7</b>	<b>8</b>	<b>10</b>	<b>11</b>	<b>12</b>	<b>14</b>
Formula	C <sub>30</sub> H <sub>39</sub> Co <sub>3</sub> N <sub>6</sub> O <sub>15</sub>	C <sub>85.5</sub> H <sub>115</sub> Fe <sub>6</sub> N <sub>23.5</sub> O <sub>28.5</sub>	C <sub>15.50</sub> H <sub>23.83</sub> Fe- N <sub>3.83</sub> O <sub>5.83</sub>	C <sub>48</sub> H <sub>67</sub> Fe <sub>3</sub> N <sub>9</sub> O <sub>12.5</sub>	C <sub>72.5</sub> H <sub>111</sub> Ga <sub>6</sub> N <sub>12</sub> O <sub>34</sub>	C <sub>35.5</sub> H <sub>55</sub> Ga <sub>3</sub> N <sub>6</sub> O <sub>17.5</sub>	C <sub>42</sub> H <sub>63</sub> Ga <sub>6</sub> N <sub>6</sub> O <sub>15</sub>	C <sub>69</sub> H <sub>117</sub> Ga <sub>3</sub> N <sub>6</sub> O <sub>15</sub>
Formula weight	900.46	2263.11	413.07	1137.66	2113.05	1055.02	1310.30	1479.85
Crystal system	triclinic	triclinic	rhombohedral	monoclinic	monoclinic	triclinic	monoclinic	triclinic
Space group	<i>P</i> $\bar{1}$	<i>P</i> $\bar{1}$	<i>R</i> $\bar{3}$	<i>C</i> 2/ <i>c</i>	<i>P</i> 2 <sub>1</sub>	<i>P</i> $\bar{1}$	<i>P</i> 2 <sub>1</sub> / <i>c</i>	<i>P</i> $\bar{1}$
Unit cell dimensions								
<i>a</i> (Å)	10.2190(8)	22.887(8)	17.925(3)	28.551(8)	18.124(2)	10.804(2)	14.523(1)	14.684(2)
<i>b</i> (Å)	12.987(1)	17.585(13)	17.925(3)	16.058(5)	13.591(2)	15.322(2)	16.946(1)	15.394(1)
<i>c</i> (Å)	14.912(2)	14.432(4)	32.770(7)	28.298(8)	34.315(5)	15.876(2)	21.584(2)	20.076(3)
$\alpha$ (°)	85.150(9)	89.90(5)	90	90	90	115.43(1)	90	70.34(1)
$\beta$ (°)	85.293(8)	109.10(2)	90	118.67(2)	94.79(1)	93.56(2)	103.321(8)	74.091(8)
$\gamma$ (°)	67.777(9)	89.88(5)	120	90	90	102.29(1)	90	74.818(1)
<i>V</i> (Å <sup>3</sup> )	1822.8(3)	5489(5)	9119(3)	11 383(6)	8423(2)	2283.7(6)	5169.0(7)	4037.1(9)
<i>Z</i>	2	2	18	8	4	2	4	2
Calc. density (mg m <sup>-3</sup> )	1.641	1.369	1.354	1.328	1.666	1.534	1.684	1.217
Absorption coefficient (mm <sup>-1</sup> )	1.427	0.852	0.779	0.819	1.987	1.833	3.152	1.054
Crystal size (mm)	0.55 × 0.28 × 0.18	0.65 × 0.30 × 0.25	0.50 × 0.30 × 0.15	0.45 × 0.30 × 0.15	0.40 × 0.30 × 0.10	0.65 × 0.40 × 0.20	0.40 × 0.30 × 0.20	0.80 × 0.50 × 0.40
$\theta$ Range for data collection (°)	1.37–19.97	0.94–22.98	1.45–22.99	1.92–20.00	1.13–23.97	1.44–23.97	1.44–14.98	1.10–23.01
Reflections collected/unique	3393/3392 [ <i>R</i> <sub>int</sub> = 0.3176]	15680/15196 [ <i>R</i> <sub>int</sub> = 0.0229]	4468/2822 [ <i>R</i> <sub>int</sub> = 0.0856]	5369/5229 [ <i>R</i> <sub>int</sub> = 0.0508]	14168/13 727 [ <i>R</i> <sub>int</sub> = 0.0470]	6259/6222 [ <i>R</i> <sub>int</sub> = 0.0005]	1633/1499 [ <i>R</i> <sub>int</sub> = 0.0216]	11 182/11 164 [ <i>R</i> <sub>int</sub> = 0.0329]
Data/restraints/parameters	3392/0/512	15 196/0/1017	2822/0/325	5229/55/712	13 727/25/1028	6222/0/608	1499/0/283	11 164/44/844
Goodness-of-fit on <i>F</i> <sup>2</sup>	1.122	1.341	1.040	1.048	1.111	1.121	1.077	1.316
Final <i>R</i> indices [ <i>I</i> > 2σ( <i>I</i> )]	<i>R</i> <sub>1</sub> = 0.0487, <i>wR</i> <sub>2</sub> = 0.1228	<i>R</i> <sub>1</sub> = 0.1093, <i>wR</i> <sub>2</sub> = 0.2707	<i>R</i> <sub>1</sub> = 0.0717, <i>wR</i> <sub>2</sub> = 0.1828	<i>R</i> <sub>1</sub> = 0.0845, <i>wR</i> <sub>2</sub> = 0.2196	<i>R</i> <sub>1</sub> = 0.0975, <i>wR</i> <sub>2</sub> = 0.2631	<i>R</i> <sub>1</sub> = 0.0647, <i>wR</i> <sub>2</sub> = 0.1594	<i>R</i> <sub>1</sub> = 0.0525, <i>wR</i> <sub>2</sub> = 0.1287	<i>R</i> <sub>1</sub> = 0.0948, <i>wR</i> <sub>2</sub> = 0.2664
<i>R</i> indices (all data)	<i>R</i> <sub>1</sub> = 0.0688, <i>wR</i> <sub>2</sub> = 0.1298	<i>R</i> <sub>1</sub> = 0.1678, <i>wR</i> <sub>2</sub> = 0.3063	<i>R</i> <sub>1</sub> = 0.1229, <i>wR</i> <sub>2</sub> = 0.2400	<i>R</i> <sub>1</sub> = 0.1272, <i>wR</i> <sub>2</sub> = 0.2632	<i>R</i> <sub>1</sub> = 0.1885, <i>wR</i> <sub>2</sub> = 0.3003	<i>R</i> <sub>1</sub> = 0.0917, <i>wR</i> <sub>2</sub> = 0.1685	<i>R</i> <sub>1</sub> = 0.0571, <i>wR</i> <sub>2</sub> = 0.1319	<i>R</i> <sub>1</sub> = 0.1386, <i>wR</i> <sub>2</sub> = 0.3461
Largest difference peak and hole (e Å <sup>-3</sup> )	0.457 and –0.283	1.374 and –0.572	0.373 and –0.422	0.466 and –0.508	1.137 and –0.631	0.808 and –0.853	0.322 and –0.287	0.732 and –1.631

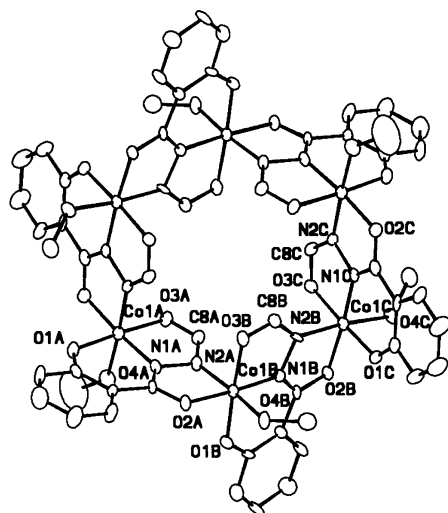


Fig. 1. An ORTEP drawing of complex **1**,  $[\text{Co}(\text{fshz})(\text{MeOH})_6]$ . A–C in cobalt ions could be related to each other using a non-crystallographic  $S_6$  symmetry operation. Hydrogen atoms have been omitted for clarity.

hole in the center of the metallamacrocycle. The approximate dimensions of the hydrophobic hole (1.95 Å) are also slightly smaller than that of the corresponding manganese complex  $[\text{Mn}(\text{fshz})(\text{DMF})_6]$  (2.70 Å) (Table 3).

Table 2

Selected bond distances (Å)<sup>a</sup> and angles (°)<sup>a</sup> for Co-metallamacrocycles **1**; and Fe-metallamacrocycles **6–8**; Ga-metallamacrocycles **10–12** and **14**; Mn-metallamacrocycles **15–19**

	<b>1</b>	<b>6</b>	<b>7</b>	<b>8</b>	<b>10</b>	<b>11</b>	<b>12</b>	<b>14</b>	<b>15</b>	<b>16</b>	<b>17</b>	<b>18</b>	<b>19</b>
M1–O1	1.862	1.889	1.893	1.895	1.914	1.901	1.90	1.899	1.852	1.851	1.859	1.852	1.858
M1–O2 <sup>c</sup>	1.906	1.982	1.995	2.002	1.947	1.932	1.97	1.938	1.967	1.967	1.971	1.973	1.967
M1–O3	1.921	2.022	2.034	2.029	2.038	2.000	1.98	1.979	1.945	1.929	1.925	1.915	1.923
M1–O4	1.946	2.050	2.064	2.104	2.027	2.074	2.08	2.088	1.929	1.942	1.93	1.935	1.932
M1–N1	1.842	2.017	2.039	2.053	1.968	1.966	2.03	1.981	2.233	2.248	2.260	2.239	2.268
M1–N2 <sup>c</sup>	1.863	2.109	2.101	2.111	2.047	2.050	2.12	2.048	2.246	2.251	2.27	2.265	2.251
O1–M1–O2 <sup>c</sup>	89.8	104.1	104.1	101.83	97.18	98.53	95.8	97.9	94.6	96.5	96.2	95.7	96.5
O1–M1–O3	177.1	161.2	161.2	161.83	168.16	169.57	174.0	170.1	169.9	170.7	170.3	170.0	170.5
O1–M1–O4	89.4	93.5	93.9	92.00	89.26	90.47	92.6	92.3	92.1	91.6	91.3	91.4	89.7
O1–M1–N1	93.9	86.3	86.1	86.37	90.84	91.27	91.7	91.8	90.5	90.8	90.6	90.5	91.0
O1–M1–N2 <sup>c</sup>	91.3	94.4	96.2	97.47	94.22	94.23	93.2	91.7	96.7	93.9	93.1	95.7	94.4
O2 <sup>a</sup> –M1–O3	92.7	94.6	94.7	96.07	93.02	91.30	92.8	91.9	95.0	92.7	93.4	93.9	92.5
O2 <sup>a</sup> –M1–O4	89.3	82.5	82.4	85.20	87.39	85.50	84.8	87.2	83.6	86.8	86.0	85.8	86.7
O2 <sup>a</sup> –M1–N1	175.6	169.3	169.3	171.40	170.45	169.37	171.1	169.7	172.7	172.5	173.0	173.4	172.3
O2 <sup>a</sup> –M1–N2 <sup>c</sup>	184.0	76.0	75.8	75.23	79.54	79.40	79.8	80.1	74.7	75.1	74.3	74.3	74.8
O3–M1–O4	89.4	89.2	88.4	86.40	88.00	87.07	86.0	86.8	86.0	88.5	88.3	86.5	88.5
O3–M1–N1	83.6	75.1	75.1	75.63	78.99	78.73	78.7	78.9	80.2	80.1	79.7	80.1	80.0
O3–M1–N2 <sup>c</sup>	90.3	89.5	88.5	90.10	90.76	90.77	90.3	90.8	88.7	88.9	89.7	89.5	90.2
O4–M1–N1	93.0	93.3	93.9	92.80	95.30	90.47	89.9	87.6	101.5	94.6	95.0	95.9	94.0
O4–M1–N2 <sup>c</sup>	173.1	159.2	157.7	159.20	165.76	164.43	163.7	167.0	157.0	161.3	159.3	159.2	161.0
N1–M1–N2 <sup>c</sup>	93.7	106.3	106.6	105.90	97.37	104.00	104.9	104.5	99.6	102.9	104.3	103.4	104.1

<sup>a</sup> The average values of chemically equivalent distances and angles.

<sup>b</sup> Ref. [7] **15**,  $[\text{Mn}(\text{fshz})(\text{MeOH})_6]$ ; **16**,  $[\text{Mn}(\text{ashz})(\text{MeOH})_6]$ ; **17**,  $[\text{Mn}(\text{pshz})(\text{MeOH})_6]$ ; **18**,  $[\text{Mn}(\text{hshz})(\text{MeOH})_6]$ ; **19**,  $[\text{Mn}(\text{lshz})(\text{MeOH})_6]$ .

<sup>c</sup> Symmetry transformations used to generate equivalent atoms.

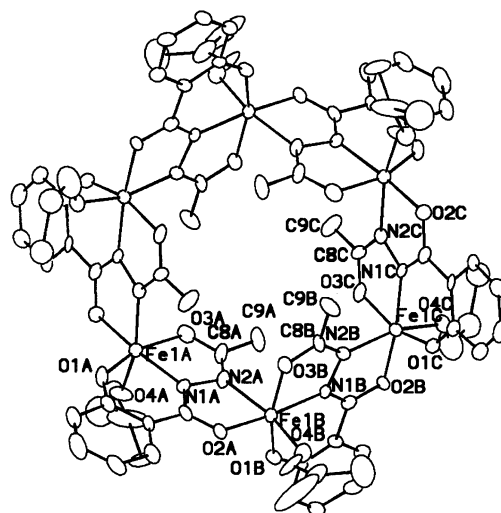


Fig. 2. An ORTEP drawing of complex **6**,  $[\text{Fe}(\text{ashz})(\text{DMF})_6]$ .

### 3.2.2. Iron-metallamacrocycles

*Crystal structure of  $[\text{Fe}(\text{ashz})(\text{DMF})_6]$  (**6**).* A hexanuclear iron-metallamacrocycle **6** could be synthesized using ferrous chloride tetrahydrate as the metal source and  $\text{ashz}^{3-}$  as a trianionic pentadentate ligand. An ORTEP diagram of complex **6** is shown in Fig. 2. The approximate dimensions of complex **6** are similar to that of the corresponding manganese complex **16** (Table 3). Complex **6** also has a vacant, hydrophobic

Table 3  
Selected distances (Å) and sizes (Å) for Co-metallamacrocycles 1, and Fe-metallamacrocycles 6–8; Ga-metallamacrocycles 10–12 and 14; Mn-metallamacrocycles<sup>a</sup> 15–19

	1	6	7	8	10	11	12	14	15	16	17	18	19
M1A...M1B <sup>b</sup>	4.427	4.890	4.902	4.909	4.722	4.722	4.722	4.706	4.805	4.819	4.891	4.880	4.877
M1A...M1C <sup>c</sup>	7.170	8.302	8.338	8.360	7.867	8.057	8.033	8.041	8.031	8.208	8.256	8.183	8.268
C8A...C8C <sup>c</sup>	4.375	5.411	5.428	5.434	5.028	5.269	5.197	5.800	5.026	5.226	5.405	5.235	5.355
C9A...C9C <sup>c</sup>	4.370	4.460	4.460	4.466	4.292	4.292	4.207	4.254	4.258	4.258	4.126	4.211	4.204
Diameter <sup>d</sup>	16.64	17.30	18.08	17.99	16.33	16.67	17.90	17.19	17.70	17.50	17.71	17.62	17.26
Thickness <sup>e</sup>	7.17	8.35	7.92	7.67	8.48	8.81	7.49	8.43	7.23	7.81	7.56	7.62	8.31
M <sub>6</sub> plane <sup>f</sup>	0.786	0.523	0.461	0.517	0.638	0.398	0.353	0.336	0.737	0.577	0.546	0.612	0.581
Ligand plane <sup>g</sup>	0.055	0.019	0.078	0.068	0.123	0.085	0.131	0.098	0.047	0.064	0.110	0.071	0.074
Dihedral angle <sup>h</sup>	55.4	51.7	47.8	48.6	57.0	52.1	46.2	49.7	50.9	49.8	45.5	50.4	51.7

<sup>a</sup> Ref. [7] 15, [Mn(ishz)(MeOH)]<sub>6</sub>; 16, [Mn(ashz)(MeOH)]<sub>6</sub>; 17, [Mn(pshz)(MeOH)]<sub>6</sub>; 18, [Mn(hshz)(MeOH)]<sub>6</sub>; 19, [Mn(ishz)(MeOH)]<sub>6</sub>.

<sup>b</sup> Distance between non-crystallographic S<sub>6</sub> symmetry-related atoms.

<sup>c</sup> Distance between non-crystallographic C<sub>3</sub> symmetry-related atoms.

<sup>d</sup> Diameter of metallamacrocycle was calculated from the distance between three C<sub>3</sub> symmetry-related phenyl hydrogen atoms of the ligand, where van der Waals radii of hydrogen atom was assumed to be 1.10 Å.

<sup>e</sup> Thickness of metallamacrocycle.

<sup>f</sup> The average value of the planarity of six ring metal ions in the metallamacrocycles in root mean square.

<sup>g</sup> The average value of the planarity of the ligand in root mean square.

<sup>h</sup> The average dihedral angle between the M<sub>6</sub> plane and the ligand plane.

hole in the center of the metallamacrocycle. The dimensions of the hydrophobic hole of complex 6 are slightly larger than that of the corresponding manganese complex [Mn(ashz)(DMF)]<sub>6</sub> (Table 3). The entrance of the hole at each face is closed by three methyl groups of the ligands. The diameter of the entrance of the hole formed by the pseudo-C<sub>3</sub> symmetry-related three methyl carbon atoms (C9) is about 1.2 Å smaller than that of the entrance of the hole formed by the pseudo-C<sub>3</sub> symmetry-related three C8 carbon atoms (Table 3).

**Crystal structure of [Fe(pshz)(DMF)]<sub>6</sub> (7).** A hexanuclear iron-metallamacrocycle 7 could be synthesized using iron(II) chloride tetrahydrate as a metal source and pshz<sup>3-</sup> as a trianionic pentadentate ligand. An ORTEP diagram of complex 7 is shown in Fig. 3. In the crystal structure of [Mn(pshz)(DMF)]<sub>6</sub> (17) one of the ethyl side chains of the ligands is located on the inside of the hole and the remaining ethyl groups are at the face of the hole [7b]. As a result, the hole size of the metallamacrocycle had expanded slightly. However, in the crystal structure of complex 7, all of the ethyl side chains of the ligands are at the face of the hole and there is no evidence of expansion of the metallamacrocycle.

**Crystal structure of [Fe(hshz)(DMF)]<sub>6</sub> (8).** A hexanuclear iron-metallamacrocycle 8 could be synthesized using ferrous chloride tetrahydrate as a metal source and hshz<sup>3-</sup> as a trianionic pentadentate ligand. An ORTEP diagram of complex 8 is shown in Fig. 4. As in the manganese-metallamacrocycle [Mn(hshz)(DMF)]<sub>6</sub> (18), complex 8 has two sets of tripled hydrophobic tails at each face of the disc-shaped metallamacrocycles [7b]. In the crystal structure, three alternating pentyl side chains are aligned approximately at a right angle to the plane of the metallamacrocycle in one direction and the other three alternating pentyl side chains are aligned in the opposite direction (Fig. 4(b)).

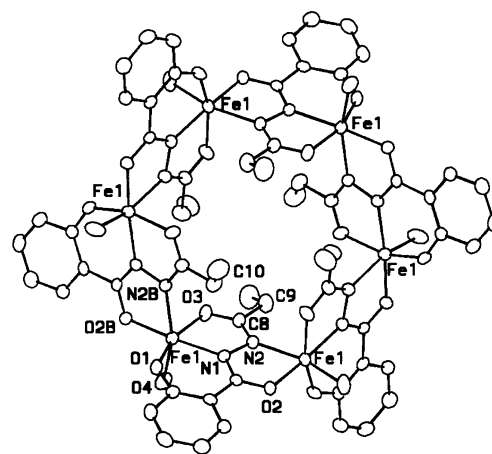


Fig. 3. An ORTEP drawing of complex 7, [Fe(pshz)(DMF)]<sub>6</sub>.

### 3.2.3. Gallium-metallamacrocycles

Crystal structure of  $[Ga(fshz)(EtOH)]_6$  (**10**)  $[Ga(ashz)(MeOH)]_6$  (**11**) and  $[Ga(pshz)(EtOH)]_6$  (**12**). The basic feature of the metallamacrocycles **10**–**12** is similar to the other corresponding hexanuclear metallamacrocycles (Tables 2 and 3). The size of the gallium-metallamacrocycles lies between those of the cobalt and manganese-metallamacrocycles.

Crystal structure of  $[Ga(lshz)(EtOH)]_6$  (**14**). An ORTEP diagram of complex **14** is shown in Fig. 5. As in the iron-metallamacrocycle  $[Fe(hshz)(DMF)]_6$ , complex **14** has two sets of tripled hydrophobic tails at each face of the donut-shaped metallamacrocycles. In the crystal structure, three alternating long alkyl side chains are aligned in the same direction, but bent. This bending might be due to the packing interaction of the hydrophobic alkyl chains.

In this study, we extended the use of metal ions in the metallamacrocycles to other octahedral transition metal ions with +3 oxidation states. We synthesized a series

of hexanuclear metallamacrocycles using various transition metal ions with +3 oxidation states as the metal source. These metallamacrocycles could be used as nanoscale building blocks for the preparation of microporous materials with various active metal sites for the recognition of the substrates. When we tried to synthesize the vanadium analogues, we could only get the linear trinuclear vanadium complexes [12].

Although there are some minor variations of geometry in the metallamacrocycles, all hexanuclear metallamacrocycles with various lengths of hydrophobic aliphatic linear chain and various metal ions are isostructural. The formation of hexanuclear metallamacrocycles is undisturbed not only by the introduction of the side chain to the ligand, but also by the change of the manganese ion to the other octahedral transition metal ions such as cobalt, iron and gallium. The isostructural metallamacrocycles containing various functional groups might have interesting properties. Five donor atoms from two chelating pentadentate

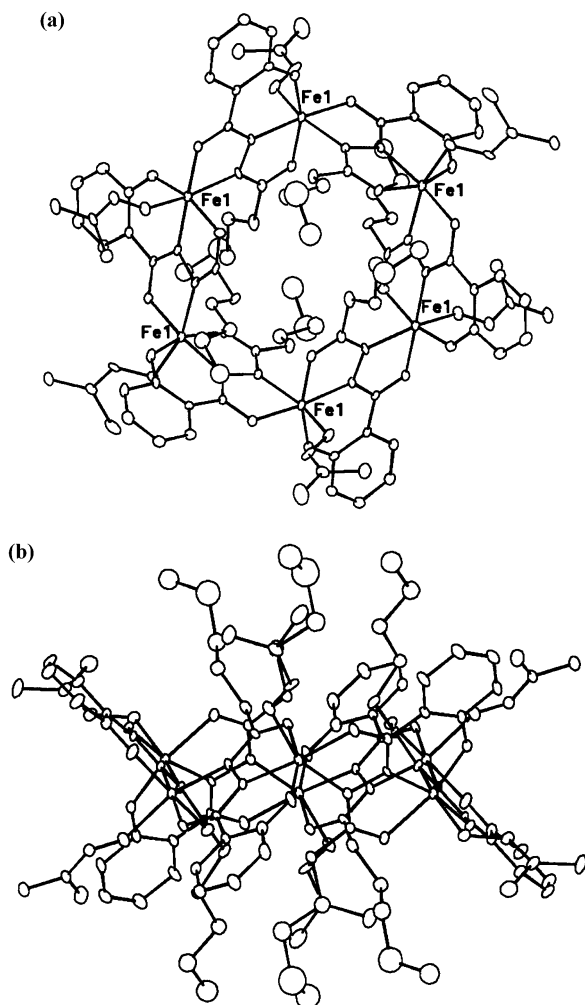


Fig. 4. (A) An ORTEP drawing of complex **8**,  $[Fe(hshz)(DMF)]_6$ ; and (B) Side view of complex **8**. The alternating side chains are aligned approximately at a right angle to the plane of the metallamacrocycle.

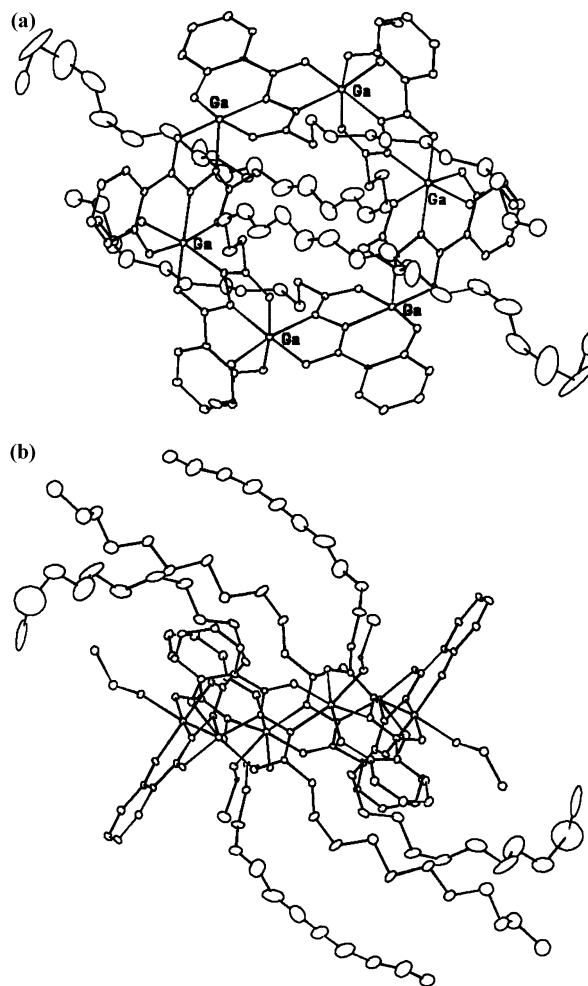


Fig. 5. (A) An ORTEP drawing of complex **14**,  $[Ga(lshz)(EtOH)]_6$ ; and (B) Side view of complex **14**. The terminal parts of the alternating long alkyl side chains were bent.



ligands and an additional donor atom from a solvent molecule have coordinated each metal center in the metallamacrocycles. The presence of this replaceable solvent site also indicates that hexanuclear metallamacrocycles could be used as nanoscale secondary building units for the preparation of open frameworks [8] with various kinds of active metal site for the recognition and the activation of guest molecules. Currently, we are expanding our studies on the synthesis and characterization of open frameworks using these building units.

#### 4. Supplementary material

Crystallographic data for the structural analysis have been deposited with the Cambridge Crystallographic Data Centre, CCDC Nos. 146711–146718. Copies of this information can be obtained free of charge from The Director, CCDC, 12 Union Road, Cambridge CB2 1EZ, UK (fax: +44-1223-336033; e-mail: deposit@ccdc.cam.ac.uk or www: <http://www.ccdc.cam.ac.uk>).

#### Acknowledgements

We thank the Korean Institute of Basic Science for elemental analyses and mass spectra, and the National Institute of Technology and Quality, Dr. Y. Park and Dr. M. Choi, for the use of their X-ray diffractometers. This work has been supported by the Korea Research Foundation (1999-015-DI0053).

#### References

- [1] (a) D. Braga, F. Grepioni, G.R. Desiraju, *Chem. Rev.* 98 (1998) 1375. (b) B. Linton, A.D. Hamilton, *Chem. Rev.* 97 (1997) 1669. (c) P.J. Stang, B. Olenyuk, *Acc. Chem. Res.* 30 (1997) 502. (d) M.J. Zaworotko, *Angew. Chem., Int. Ed. Engl.* 37 (1998) 1211. (e) C. Janiak, *Angew. Chem., Int. Ed. Engl.* 36 (1997) 1431.
- [2] (a) T. Ezuhara, K. Endo, Y. Aoyama, *J. Am. Chem. Soc.* 121 (1999) 3279. (b) C.V.K. Sharama, G.A. Broker, J.G. Huddleston, J.W. Baldwin, R.M. Metzger, R.D. Rogers, *J. Am. Chem. Soc.* 121 (1999) 1137. (c) Y.M. Jeon, J. Kim, D. Whang, K. Kim, *J. Am. Chem. Soc.* 118 (1996) 11333. (d) Y.-B. Dong, R.C. Layland, M.D. Smith, N.G. Pschirer, U.H.F. Bunz, H.-C. Loye, *Inorg. Chem.* 38 (1999) 3056.
- [3] (a) S.W. Keller, S. Lopez, *J. Am. Chem. Soc.* 121 (1999) 6306. (b) W. Lin, O.R. Evans, R. Xiong, Z. Wang, *J. Am. Chem. Soc.* 120 (1998) 13272. (c) H.J. Choi, M. Suh, *J. Am. Chem. Soc.* 120 (1998) 10622. (d) L.R. MacGillivray, R.H. Groeneman, J.L. Atwood, *J. Am. Chem. Soc.* 120 (1998) 2676. (e) D. Whang, K. Kim, *J. Am. Chem. Soc.* 119 (1997) 451. (f) D. Venkatarman, G.B. Gardner, S. Lee, J.S. Moore, *J. Am. Chem. Soc.* 117 (1995) 11600. (g) G.K.H. Shimizu, G.D. Enright, C.I. Ratcliffe, J.A. Ripmeester, D.D.M. Wayner, *Angew. Chem., Int. Ed. Engl.* 37 (1998) 1407. (h) J. Li, H. Zeng, J. Chen, Q. Wang, X. Wu, *Chem. Commun.* (1997) 1213.
- [4] (a) D.V. Soldatov, J.A. Ripmeester, S.I. Shergina, I.E. Sokolov, A.S. Zanina, S.A. Gromilov, Y.A. Dyadin, *J. Am. Chem. Soc.* 121 (1999) 4179. (b) T.M. Reineke, M. Eddaoudi, M. Fehr, D. Kelley, O.M. Yaghi, *J. Am. Chem. Soc.* 121 (1999) 1651. (c) O.M. Yaghi, C.E. Davis, G. Li, H. Li, *J. Am. Chem. Soc.* 119 (1997) 2861. (d) G.B. Gardner, Y.-H. Kiang, S. Lee, A. Asgaonkar, D. Venkataraman, *J. Am. Chem. Soc.* 118 (1996) 6946. (e) B.F. Abrahams, P.A. Jackson, R. Robson, *Angew. Chem., Int. Ed. Engl.* 37 (1998) 2656. (f) T.L. Hennigar, D.C. MacQuarrie, P. Losier, R.D. Rogers, M.J. Zaworotko, *Angew. Chem., Int. Ed. Engl.* 36 (1997) 972. (g) P. Losier, M.J. Zaworotko, *Angew. Chem., Int. Ed. Engl.* 35 (1996) 2779. (h) A.M. Ibrahim, E. Siebel, R.D. Fischer, *Inorg. Chem.* 37 (1998) 3521.
- [5] (a) H. Gudbjartson, K. Biradha, M. Poirier, M.J. Zaworotko, *J. Am. Chem. Soc.* 121 (1999) 2599. (b) S.R. Batten, B.F. Hoskins, R. Robson, *J. Am. Chem. Soc.* 117 (1995) 5385. (c) G.B. Gardner, D. Venkataraman, J.S. Moore, S. Lee, *Nature* 374 (1995) 792. (d) M. Kondo, T. Yoshitomi, K. Seki, H. Matsuzaka, S. Kitagawa, *Angew. Chem., Int. Ed. Engl.* 36 (1997) 1725. (e) O.R. Evans, Z. Wang, R.-G. Xiong, B.M. Foxman, W. Lin, *Inorg. Chem.* 38 (1999) 2969.
- [6] (a) S.S.-Y. Chui, S.M.-F. Lo, P.H. Charmant, A.G. Orpen, I.D. Williams, *Science* 283 (1999) 1148. (b) H. Li, A. Laine, M. O'Keeffe, O.M. Yaghi, *Science* 283 (1999) 1145.
- [7] (a) B. Kwak, H. Rhee, S. Park, M.S. Lah, *Inorg. Chem.* 37 (1998) 3599. (b) B. Kwak, H. Rhee, M.S. Lah, *Polyhedron* 19 (2000) 1985.
- [8] M. Moon, I. Kim, M.S. Lah, *Inorg. Chem.* 39 (2000) 2710.
- [9] G.M. Sheldrick, *Acta Crystallogr., Sect. A* 46 (1990) 467.
- [10] G.M. Sheldrick, *SHELX-97*, University of Göttingen, Göttingen, Germany, 1997.
- [11] A.L. Spek, *Acta Crystallogr., Sect. A* 46 (1990) 194 (PLATON program).
- [12] M. Moon, M.S. Lah, unpublished result.